Available online at www.sciencedirect.com
ScienceDirect
Journal of Magnetism and Magnetic Materials 307 (2006) 186–190
Journal of magnetism and magnetic materials
www.elsevier.com/locate/jmmm

Unveiling instability in Cr-doped $Nd_{0.5}Ca_{0.5}MnO_3$

Jiyu Fan, Li Pi, Yuheng Zhang*

Hefei High Magnetic Field Laboratory, University of Science and Technology of China, Hefei 230026, Anhui, People's Republic of China

Received 5 September 2005; received in revised form 25 March 2006
Available online 2 May 2006

Abstract

The magnetic phase transition and insulating-metal phase transition in the charge ordering (CO) $Nd_{0.51}Ca_{0.49}Mn_{0.98}Cr_{0.02}O_3$ system have been studied. From the magnetization and resistivity measurements, a considerable instability is observed in the temperature region $40\,K \leqslant T \leqslant 135\,K$ upon thermal cycle. In the thermal hysteresis region, both antiferromagnetic (AFM) and paramagnetic (PM) phases transform into ferromagnetic (FM) phase as the temperature decreases, thus the strong ferromagnetism emerges in the system. The origin of the instability should be attributed to the strain relaxation in the interfacial region. Interestingly, due to the growing FM interaction, the AFM coupling becomes weakened rather than strengthened at low temperatures.

PACS: 75.47.Lx; 75.60.Ej; 71.30.+h

Keywords: Perovskite manganites; Instability; Ferromagnetism

1. Introduction

Mixed-valence perovskite manganites $R_{1-x}A_xMnO_3$ (R = rare-earth element, A = divalent alkaline earth element) with colossal magnetoresistance effect have been of great interest in the past years due to their special electronic and magnetic properties as well as the potential ability for application [1–3]. Extensive studies have shown that the local inhomogeneity and the competitions between different phases play a crucial role in these compounds [4–6]. It is well-confirmed that, the charge ordering/orbital ordering (CO/OO) for $x = 0.5$ hole-doped manganites behaves as the periodic arrangement of Mn^{3+} and Mn^{4+} ions. As a typical material, $Nd_{0.5}Ca_{0.5}MnO_3$ (NCMO) undergoes a CO transition at $T_{CO} = 250\,K$ and the antiferromagnetic (AFM) ordering transition at $T_N = 160\,K$ [7]. The experiments reveal that a few Cr impurities substitution can cause the CO/OO collapse and reproduce some ferromagnetic (FM) metallic clusters in AFM insulating matrix [8–10]. Interestingly, a special instability, namely, magnetic and transport properties depending on thermal cycling, has been found in the CO system [11]. From the past work, it is easy to find that the instability always occurs in the temperature region $T < T_{CO}$, and is strongly correlated to short-range/local CO state [12]. Although there are already some reasonable explanations to that, full understanding of this behavior is lacking mainly due to its complexity and the difficulty in directly observing its kinetic process. Therefore, we suppose, if the previous long-ranged CO phase could be partly damaged and simultaneously, abundant short-range CO phase could easily appear, it will be in favor of the study. Accordingly, in this paper, we substitute Mn^{3+} ions with Cr^{3+} ions to synthesize $Nd_{0.51}Ca_{0.49}Mn_{0.98}\ Cr_{0.02}O_3$ (NCMCO) compound with a fixed ratio of $Mn^{3+} : Mn^{4+} = 1 : 1$. Obviously, this doping method settles one common issue in the conventional Cr-doped method, which changes the Mn^{3+}/Mn^{4+} ratio and thus affects the CO/OO formation. As we expected, the instability not only occurs in the current system but also behaves more distinctly than the previous reports. From the magnetization and resistivity measurement, an appreciable thermal magnetic hysteresis is observed in NCMCO compounds. The resistivity is increasing with time until the end of 14th thermal cycle. From the results of the M-H loop and electron-spin-resonance (ESR) spectra, it has

*Corresponding author. Tel.: +86 5113602808; fax: +86 5513602803.
E-mail address: zhangyh@ustc.edu.cn (Y. Zhang).

0304-8853/$ - see front matter © 2006 Elsevier B.V. All rights reserved.
doi:10.1016/j.jmmm.2006.04.001

been found that the AFM coupling becomes weakened and therefore the AFM phase transforms into the FM phase at $T<100$ K. Both paramagnetic (PM)–FM and AFM–FM phases transition result in the strong ferromagnetism at low temperatures.

2. Experiment

Polycrystalline NCMCO sample was prepared by the conventional solid-state reaction method with high-purity Nd_2O_3, $CaCO_3$, MnO_2 and Cr_2O_3 as the starting materials. The mixture was preheated in air at 900 °C for 24 h. Afterwards the powder was ground and heated at 1200 °C for 30 h. Finally, it was reground, pressed into pellets and sintered for another 40 h at 1400 °C, and was cooled down to room temperature with the furnace. The structure and phase purity has been checked by X-ray powder diffraction. The sample is single phased and exhibits the orthorhombic structure. The magnetization (M) measurement was performed using a Lake-Shore vibrating sample magnetometer under 0.01 T magnetic field from 5 to 300 K. The M–H hysteresis were performed with sweep field from 6 to −6 T at different temperatures. The ESR spectra were obtained from a JES-FA200 spectrometer at 9.06 GHz. The resistivity was measured by standard four-probe method.

3. Results and discussion

Fig. 1 shows the temperature dependence of resistivity (ρ–T) curves. Every thermal cycling process is performed firstly from room temperature down to low temperature, then back to room temperature. Such a thermal cycling process is repeated for 14 times. It is found that the resistivity remarkably increases after each thermal cycling, revealing the fact that transport properties depend on thermal cyclings. At the same time, insulator–metal (I–M) transition occurs in the vicinity of 113 K for cooling process and 126 K for heating process, respectively. Such an (I–M) transition is generally thought to be a percolation-like (I–M) transition [11]. Two unusual features are worth noticing: (i) the ρ–T curve in cooling process does not overlap that in heating process in a certain region; (ii) the resistivity stops increasing since the 14th cycling. The inset of Fig. 1 is the magnified image of the first cycling process. As it shows, the cooling and heating curves superpose only in the temperature regions of $T\leqslant 39.5$ K and $T\geqslant 133$ K. In the temperature regions of $39.5\text{ K}<T<133$ K, the system presents considerable thermal hysteresis of resistance, exhibiting a character of first-order phase transition.

The temperature dependence of magnetization (M–T) for NCMCO sample is presented in Fig. 2. The first M–T curve, which is initially cooled down to 5 K without external magnetic field, is measured under 0.01 T with heating to 300 K. Then, under the same magnetic field, the second curve is recorded by decreasing temperature down to 5 K. Finally, the third curve is measured with heating up to 300 K again. For the first curve under zero-field cooling (ZFC), the M value hardly changes as the temperature changes from 300 K down to 150 K. Afterwards, however, the M increases swiftly and reaches its maximum at $T=70$ K. As the temperature further decreases from 40 to 5 K, the M decreases slightly. From the magnified M–T curve in the inset of Fig. 2, we can see an obvious bump on the first curve at $T\sim240$ K, which corresponds to the onset temperature of CO/OO. Therefore, the current doping manner can assure the formation of CO phase. Comparing the second curve with the first curve, a considerable magnetic hysteresis is found in the temperature region of $40\text{ K}\leqslant T\leqslant 135$ K, which is consistent with the thermal hysteresis in the temperature region of 39.5–133 K in the

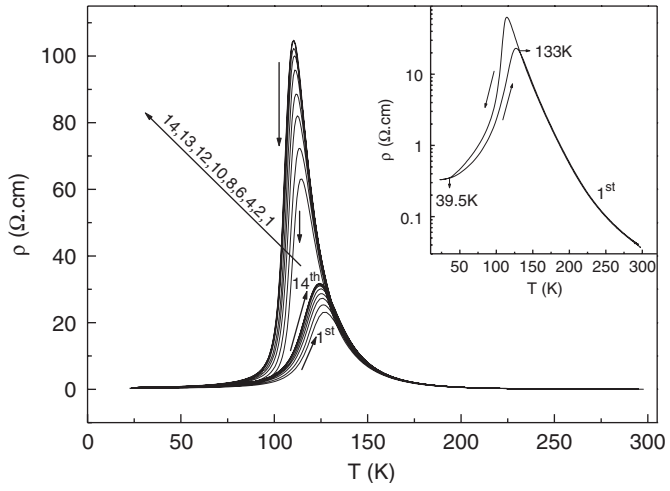

Fig. 1. Temperature dependence of resistivity for total 14 times cycling runs in $Nd_{0.51}Ca_{0.49}Mn_{0.98}Cr_{0.02}$ O_3. The inset is the magnification of first cycling run.

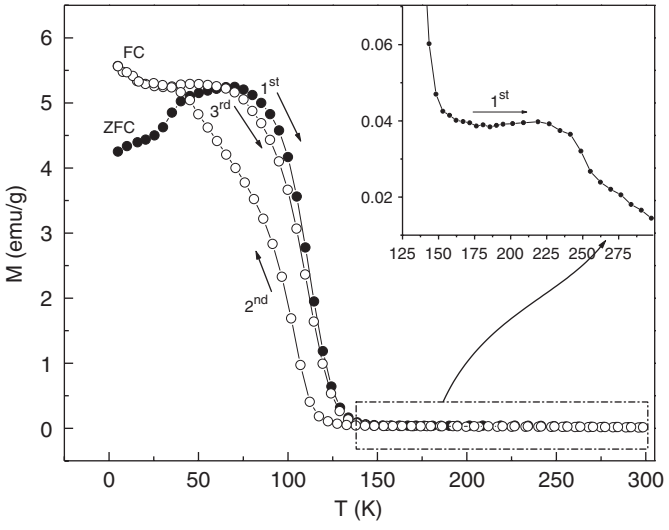

Fig. 2. Temperature variation of the magnetization of $Nd_{0.51}Ca_{0.49}Mn_{0.98}Cr_{0.02}O_3$; The first and third curves are measured in heating process, and the second in cooling process. The inset is the magnification of first curve at $125\text{ K}\leqslant T\leqslant 300$ K.

ρ–T curve. In addition, the M value in the second measurement is obviously smaller than those in the first and third processes. Comparing the third curve with the first curve, we find that the first M is slightly bigger than the third one in the temperature region of $70\,K \leqslant T \leqslant 150\,K$ showing that the magnetization decreases with the thermal cycle going on.

Based on the observed results above, we can find that the thermal cycling strongly affects the magnetic properties. In order to shed additional light onto the magnetic hysteresis region, the M–H relation is performed at special temperatures as shown in Fig. 3. At $T = 250\,K$, the M increases linearly as H increases from -6 to 6 T, showing a feature of PM phase. Since $T = 150\,K$, a small high-field loop emerges, indicating a formation of AFM phase. However, such a high-field loop only appears in the $H > 2.25\,T$ region. As the temperature decreases, the area of hysteresis loop is enlarged, but the onset of loop occurrence is driven to a low-field region (at 0.95, 0.45 and 0.35 T for 135, 115 and 100 K, respectively), indicating that the AFM phase continually grows up while AFM coupling gradually decreases. Moreover, at 115 and 100 K, we notice that the magnetization has reached saturation before applying the maximal field 6 T (saturation at 5.25 and 5.0 T for 115 and 100 K, respectively). At 65 K, the area of hysteresis loop becomes smaller, but the onset of loop occurrence moves to lower field $H = 0.15\,T$. Therefore, not only does the AFM coupling continues to get weaker but also the AFM phase decreases. At 40 and 5 K, with sweep field up to 0.5 T, the M increases rapidly and, gets saturated as $H > 0.5\,T$ exhibiting a complete FM feature. In the down-sweep process, the M–H curve basically superposes that of up-sweep process and not even a tiny high-field loop has been observed from these two curves, which implies that there is a very little amount of AFM phase in the FM background.

The inset of Fig. 3 shows the temperature dependence of the saturation magnetization (M_s). We can find that the M_s increases as the temperature decreases from 250 to 65 K while basically keeps constant at $T \leqslant 65\,K$. In the present system, all the Nd^{3+}, Mn^{3+}, Mn^{4+} and Cr^{3+} ions are magnetic ions. Therefore, it is natural to consider whether all of them contribute to magnetization. If Nd^{3+} ions' moment could be polarized under 6 T field, the theoretical saturation magnetization M_s ($= 178.64\,emu/g$) should include the contribution of all the ions. In contrast, if it could not be polarized, the saturation magnetization M_s ($= 128.73\,emu/g$) should exclude the Nd^{3+} ions' contribution. In Fig. 3, the experimental data show $M_s = 129.62\,emu/g$. Therefore, the increase of ferromagnetism should originate from Mn^{3+}, Mn^{4+} and Cr^{3+} ions, excluding Nd^{3+} ions. That is to say, the Nd^{3+} ions have not been polarized. In fact, the doubling exchange interaction between Mn^{3+}–O–Mn^{4+} and the superexchange interaction between Mn^{3+}–O–Cr^{3+} are responsible for the increase of magnetization. Nd^{3+}–O–Nd^{3+} cannot produce any interaction to form FM phase, that is, the magnetic moment of Nd^{3+} ions does not contribute to M_s.

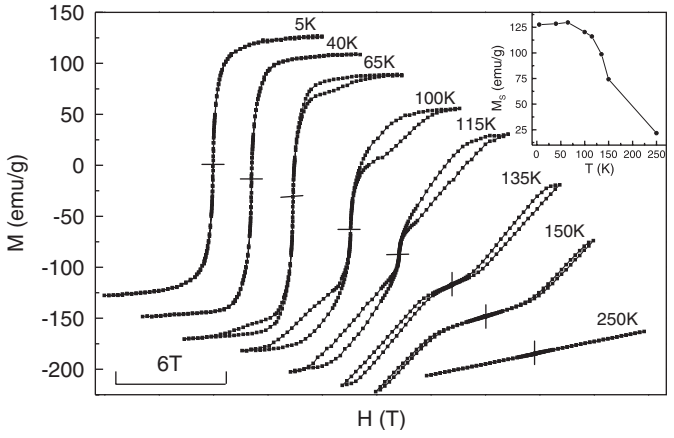

Fig. 3. The M–H loops at various temperatures for $Nd_{0.51}Ca_{0.49}Mn_{0.98}Cr_{0.02}O_3$. The inset shows the temperature dependence of the saturation magnetization (M_s).

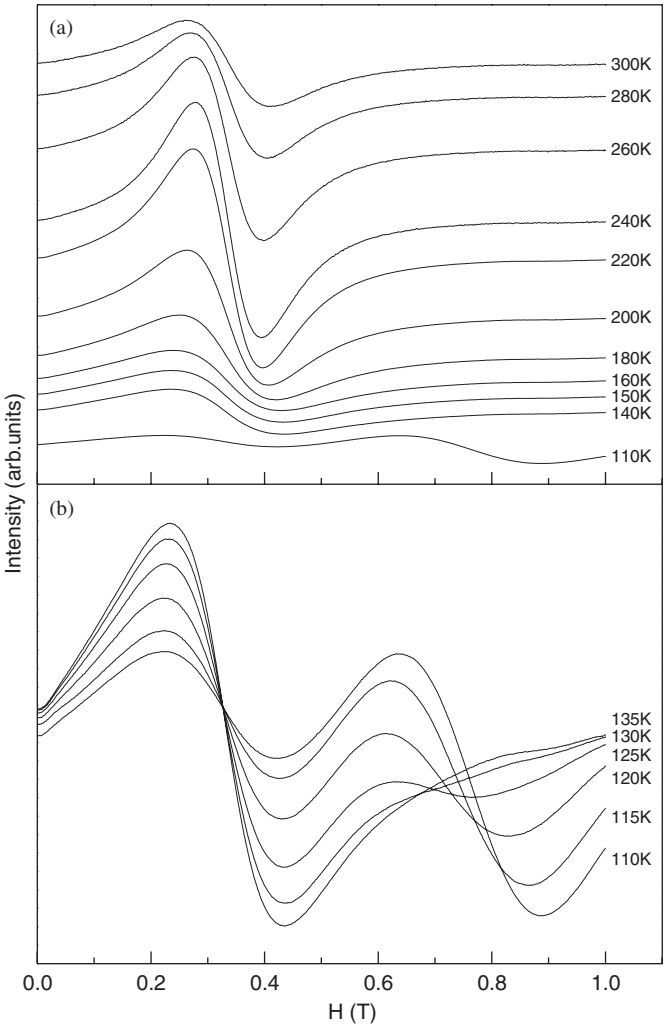

Fig. 4. Electronic spin resonance spectra of $Nd_{0.51}Ca_{0.49}Mn_{0.98}Cr_{0.02}O_3$ at different temperatures.

ESR is a powerful probe to investigate microscopic magnetic state/ordering. Hence, ESR spectra at different temperatures (300–110 K) are shown in Fig. 4(a). As temperature decreases from 300 to 240 K, the intensity of PM lines with $g\sim2$ at $H\sim0.32$ T gradually becomes stronger. Once below 240 K, however, the intensity of PM lines is weakened quickly indicating a formation of AFM phase. From Fig. 4(a), it is also discovered that PM line nearly disappears at 110 K but another stronger signal appears at $H\sim0.72$ T. In order to explain this variation, we performed ESR measurement in the temperature region of 135–110 K with a decrease step of 5 K. The magnified image is shown in Fig. 4(b). We find that the PM lines are distorted in high-field region. Two remarkable Lorentz lines occur at 125–110 K: one is PM line with $g\sim2$; the other is at high field about 0.72 T region with $g<2$, which should be the sign of weak AFM line. Moreover, with the temperature decreasing, the additional AFM signals become stronger and the PM signals become weaker. In fact, at $T>140$ K, there has been a considerable AFM phase in the system, but it has not been detected from ESR spectra. From M–H curve at 150 K (Fig. 3), we find that a hysteresis loop occurs at 2.25 T which is far above our ESR maximal sweep field (1 T). On the contrary, at 135 K, the site of the hysteresis loop is driven to 0.95 T (below 1 T). Accordingly, the AFM signal has been detected in ESR spectra. Therefore, based on M–T, M–H and ESR results, the magnetic transition can be roughly divided into three parts: charge disordering PM phase (above 240 K); CO PM phase and AFM phase (240–140 K); CO PM, FM and AFM phase (135–110 K).

The Cr^{3+} substitution induces the local inhomogeneity and some nanometer FM clusters. The multiphase coexistence and competitions govern the intricate magnetic transitions in the present system. In Fig. 3, a noticeable high-field loop is observed at 150 K but the loop occurs only in the high-field region ($H>1$ T) implying that the AFM coupling is very strong. On the contrary, it shifts to low-field region ($H<1$ T) at $T=135$ K indicating that the AFM coupling is weakened. Furthermore, the high-field loop disappears at 40 and 5 K. Therefore, in the present system, not only charge-disordering region but also CO domain takes part in magnetic transition. From the inset of Fig. 3, one can find that the saturation magnetization M_s exhibits a rapid increase at the temperature region of $65\,\text{K}<T<135$ K. At this moment a doubt rises: how does FM transition develop, from PM or AFM? To clarify it, we must investigate the evolutional process of M–H curves below 135 K. At 115 K, one can find that the PM phase has gradually disappeared and only the FM and AFM phases are remained. In order to explore the magnetic transition more clearly around 115 K, the M–H curves are fitted by using Langevin function at 115 and 100 K. We expect to separate FM contribution from the total magnetization curve, in order that, the residential part can be attributed to the PM and AFM components. It is assumed that all the FM clusters are of the same size and there is no interaction among them. Thus, every FM cluster can be considered as a single large magnetic moment. The simple model may be expressed by

$$M = Nm\mu L\left(\frac{m\mu H}{k_B T}\right),$$

where $L(m\mu H/k_B T)$ is the Langevin function; N is the number of FM clusters in one mole of the NCMCO; m is the number of $Mn^{3+/4+}$ ions in a FM cluster; $\mu = 3.5\,\mu_B$ is the average magnetic moment of $Mn^{3.5+}$ (μ_B is Bohr magneton). The M–H curve in the low-field region is fitted by the Langevin function so that the FM magnetization curve can be calculated in the whole sweep field range. Finally, the FM magnetization curve is subtracted from the experimental magnetization curve to get net contribution of the PM and AFM phase as shown in Fig. 5.

From the results in Fig. 5, we can find that there is a small portion of PM phase at 115 K, instead, no PM phases can be observed at 100 K indicating that the PM phase has completely transformed into the FM phase from 115 to 100 K. Such a PM–FM transition is in agreement with a slight ESR PM signal at 110 K and the rapid increase of magnetization below 135 K. Moreover, it has also been found that the onset of M–H loop at 100 K is lower than that at 115 K, exhibiting that AFM interaction has been weakened with the temperature decreasing. In the temperature region $T<100$ K, the AFM phase begins to decrease and the AFM phase transforms to the FM phase, which also contributes to the increase of the systemic magnetization. Down to 65 K, M–H curve has been nearly dominated by the FM phase only with a little AFM component. Consequently, at lower temperature 40 and 5 K, the residual AFM phase also transforms into the FM phase and thus the system exhibits pure FM behavior at the lowest temperature.

The enhancement of resistance and the diminution of the FM phase upon the thermal cycling reflect a fact that the present system is an unstable one. From the results above and other groups' work, we have found that the occurrence of instability is determined by two preconditions: (i) the unstable state always occurs in the region of PM/AFM–FM transition; (ii) some short-range/local CO phases exist. Therefore, we propose the following scenario for understanding it. As the Cr^{3+} ions are doped into

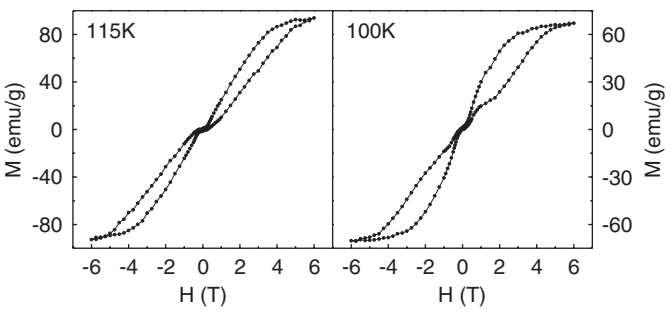

Fig. 5. The subtracted curves of M–H loops at 115 and 100 K.

NCMO, the CO and charge-disordering domains coexist in one system. In the temperature region of $T < T_{CO}$, the spin arrangement appears to be AFM ordering in the CO domain. Therefore, the AFM phase in the CO region and the PM phase in the charge-disordering region coexist in the system. Podzorov et al. [13] proposed that the CO domains do not show a noticeable change even when the system is cooled to below the I–M transition temperature in term of observation from polarized optical microscopy. It indicates that as the temperature decreases, the charge disordering region does not penetrate into the CO region. Since the double exchange between Mn^{3+} and Mn^{4+} ions can form FM coupling in the charge-disordering region, namely, the observed PM–FM phase transition occurs in the first cooling and the system becomes FM and AFM coexistence. This coexistence can result in two effects: (i) with the decrease of temperature, the strong interaction (strain) occurs in their interface because of the micro-structural difference between the AFM CO domains and the FM charge-disordering domains [14]. In heating process, the FM coupling decreases since the spins are ''frozen'' in the strain region. Thus, the PM–FM (cooling) and the FM–PM (heating) phase transitions are irreversible. (ii) The strain will prevent the charge-disordering region from transforming into FM phase and thus impede the formation of percolating path. Through thermal cycling, the accumulative strain in interfacial region gradually relaxes and the interfacial region continuously expands resulting in the enhancement of resistance and the diminution of FM phase. Due to the FM formation, the AFM coupling can be weakened by the inner magnetic field. As the temperature decreases, the enhancement of FM phase destroys AFM coupling so that the AFM phase gradually transforms to FM phase. Consequently, the strong ferromagnetism occurs at low temperatures.

Although the colossal magnetoresistance effect is extensively attributed to the double exchange interaction and Jahn–Teller effect, [15,16] the accumulated experimental evidence indicates that the ground state is not a single phase but a mixed phase, where a FM metallic phase coexists with an AFM insulating phase at low temperatures. This coexistence is usually understood within the framework of phase separation owing to correlated disorder [17]. However, recent investigations show that long-ranged strain is important. Ahn et al. proposed that the microscopic multiphase is not only self-organized behavior but caused by the presence of intrinsic strain [18]. Here, our experimental results show that the strain accumulation and relaxation play an important role in manganites, that is to say, the competition between different phases should be useful to understand the CMR effect.

4. Conclusion

In summary, the magnetic and transport properties of NCMCO were studied. With the decrease of temperature, a percolation-like I–M transition appears. From 135 to 100 K, the PM phase starts to transform into the FM phase and then the AFM phase transforms into the FM phase. The instability should be attributed to the strain relaxation which causes the decrease of FM phase and the resistivity enhancement upon thermal cycling. The inner magnetic field destroys AFM coupling which causes the magnetic variation in the CO domains.

Acknowledgements

One of the authors Jiyu Fan would like to thank his friends Dr. Wei Tong and Dr. Kuang He for a valuable discussion. This work was supported by the National Nature Science Foundation of China (nos. 10334090 and 10504029) and, by the State Key Project of Fundamental Research of China (001CB610604).

References

[1] R. von Helmolt, J. Wecker, B. Holzapfel, L. Schultz, K. Samwer, Phys. Rev. Lett. 71 (1993) 2331.
[2] S. Jin, T.H. Tiefel, M. McCormack, R.A. Fastnacht, R. Ramesh, L.H. Chen, Science 264 (1994) 413.
[3] K. Chahara, T. Ohno, M. Kassai, Y. Kozono, Appl. Phys. Lett. 63 (1993) 1990.
[4] A. Moreo, S. Yunoki, E. Dagotto, Science 283 (1999) 2034.
[5] M. Tokunaga, N. Miura, Y. Tomioka, Y. Tokura, Phys. Rev. 57 (1998) 5259.
[6] C. Kapusta, P.C. Riedi, M. Sikora, M.R. Ibarra, Phys. Rev. Lett. 84 (2000) 4216.
[7] F. Millange, S. de Brion, G. Chouteau, Phys. Rev. B 62 (2000) 5619.
[8] W. Schuddinck, G. Van Tendeloo, A. Barnabe, M. Hervieu, B. Raveau, J. Solid State Chem. 148 (1999) 333.
[9] T. Kimura, R. Kumai, Y. Okimoto, Y. Tomioka, Y. Tokura, Phys. Rev. B 62 (2000) 15021.
[10] S. Mori, R. Shoji, N. Yamamoto, T. Asaka, Y. Matsui, A. Machida, Y. Moritomo, T. Katsufuji, Phys. Rev. B 67 (2003) 012403.
[11] R. Mahendiran, B. Raveau, M. Hervieu, C. Michel, A. Maignan, Phys. Rev. B 64 (2001) 064424.
[12] R. Mahendiran, A. Maignan, M. Hervieu, C. Martin, B. Raveau, J. Appl. Phys. 90 (2001) 2422.
[13] V. Podzorov, B.G. Kim, V. Kiryukhin, M.E. Gershenson, S.-W. Cheong, Phys. Rev. B 64 (2001) 140406(R).
[14] P.G. Radaelli, D.E. Cox, M. Marezio, S.-W. Cheong, P.E. Schiffer, A.P. Ramirez, Phys. Rev. Lett. 75 (1995) 4488.
[15] C. Zener, Phys. Rev. 82 (1951) 403.
[16] A.J. Millis, P.B. Littlewood, B.J. Shraiman, Phys. Rev. Lett. 74 (1995) 5144.
[17] E. Dagotto, T. Hotta, A. Moreo, Phys. Rep. 344 (2001) 1.
[18] K.H. Ahn, T. Lookman, A.R. Bishop, Nature 428 (2004) 401.